

SSTD: Stripe-Like Space Target Detection using Single-Point Supervision

Zijian Zhu^{1,2,3,4}, Ali Zia^{5,*}, Xuesong Li⁵, Bingbing Dan^{1,2,4}, Yuebo Ma^{1,2,3,4}, Enhai Liu^{1,2,3,4}, and Rujin Zhao^{1,2,3,4,*}

¹ National Key Laboratory of Optical Field Manipulation Science and Technology, Chinese Academy of Sciences, Chengdu, China

² Institute of Optics and Electronics, Chinese Academy of Sciences, Chengdu, China

³ Key Laboratory of Science and Technology on Space Optoelectronic Precision Measurement, Chinese Academy of Sciences, Chengdu, China

⁴ University of Chinese Academy of Sciences, Beijing, China

⁵ Australian National University, Australia

Abstract. Stripe-like space target detection (SSTD) plays a key role in enhancing space situational awareness and assessing spacecraft behaviour. This domain faces three challenges: the lack of publicly available datasets, interference from stray light and stars, and the variability of stripe-like targets, which complicates pixel-level annotation. In response, we introduce ‘AstroStripeSet’, a pioneering dataset designed for SSTD, aiming to bridge the gap in academic resources and advance research in SSTD. Furthermore, we propose a novel pseudo-label evolution teacher-student framework with single-point supervision. This framework starts with generating initial pseudo-labels using the zero-shot capabilities of the Segment Anything Model (SAM) in a single-point setting, and refines these labels iteratively. In our framework, the fine-tuned StripeSAM serves as the teacher and the newly developed StripeNet as the student, consistently improving segmentation performance by improving the quality of pseudo-labels. We also introduce ‘GeoDice’, a new loss function customized for the linear characteristics of stripe-like targets. Extensive experiments show that the performance of our approach matches fully supervised methods on all evaluation metrics, establishing a new state-of-the-art (SOTA) benchmark. Our dataset and code will be made publicly available.

Keywords: Stripe-like Space Target Detection · Strong Stray Light · Single-point Weak Supervision · Pseudo-label Evolution

1 Introduction

In the evolving landscape of global space activities, the exponential increase in the number of space targets, encompassing spacecraft, space debris, and asteroids of significant astronomical interest, underscores the critical importance of space

* Corresponding authors.

target detection. Although long-term and challenging, this task is essential for the safe operation of spacecraft and the effective monitoring and management of space debris. It provides crucial technical support for space remote sensing applications, including debris mitigation, long-distance laser communications, and asteroid exploration [30, 46, 50].

High-precision and high-resolution optical telescopes, necessitated by the vast distances between space targets and observational equipment, have become the instruments of choice [26, 42, 56]. These telescopes capture space targets as stripes or Gaussian points within their field of view, with the specific outcome dependent on the operational mode (either target tracking or star tracking) and the duration of exposure [28, 29]. Extended exposure times, especially in star tracking mode, enhance the detection of space targets, presenting them as stripes due to their motion [26]. However, this advantage is counterbalanced by an increased vulnerability to space stray light interference during long exposures, which significantly compromises the signal-to-noise ratio (SNR) of stripe-like targets, as shown in Figure 1. Despite the maturity of research on point-like space target detection, as evidenced by a variety of methodologies ranging from multi-frame approaches based on motion characteristics to CNN-based methods [9, 25, 39, 45, 52, 55], the exploration of stripe-like space target detection remains nascent. This area faces several challenges:

Dataset Availability: The lack of a unified, open source, and large-scale dataset has been a significant obstacle in advancing stripe-like target detection research. The difficulty and high cost of acquiring real space images have led to a shortage of data for thoroughly benchmarking detection algorithms.

Space Noise Interference: The detection of stripe-like space targets is significantly challenged by the low SNR, a result of interference from various sources of space stray light and the presence of numerous stars [2, 4, 51], as shown in Figure 1. This interference complicates the label annotation process for data-driven methods [2].

Target Variability: The variability in the appearance of stripe-like targets, including differences in position, scale, direction, and brightness distribution, poses a challenge to traditional detection methods, necessitating more adaptable and robust approaches [7, 26].

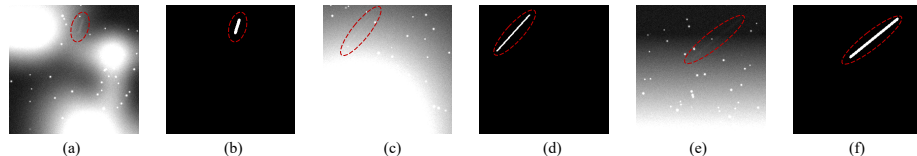


Fig. 1: Challenges in SSTD. (a), (c) and (e) show space images with different stray light, while (b), (d) and (f) are the stripe-like target's ground truths.

Despite its challenges, the investigation into stripe-like space target detection holds significant promise for enhancing space surveillance and research capabili-

ties. To address the first challenge of scarcity of public datasets suitable for deep learning research in stripe-like space target detection, we have developed the AstroStripeSet dataset. To the best of our knowledge, this dataset is the first of its kind and comprises synthesized images under various stray light scenarios accompanied by annotations in multiple formats. This initiative fills a critical gap in the domain of SSTD under stray light conditions, providing a foundational resource for benchmarking and advancing research in this field. Given the prohibitive time and resource requirements of pixel-level labeling for large-scale data, we turned our attention to the potential of foundation models, which have garnered widespread interest across various domains. Notably, models such as DINO [1, 33] and SAM [19] in computer vision have demonstrated remarkable zero-shot capabilities. These models are pre-trained on extensive datasets, enabling them to learn general pattern features and exhibit strong performance in downstream tasks without requiring task-specific training.

The emergence of foundation models in computer vision, particularly those with enhanced scene generalization capabilities like SAM, suggests a promising avenue for addressing the detection of stripe-like space targets amidst strong stray light. However, adapting these models to specialized domains such as space images remains a challenge, necessitating fine-tuning strategies to effectively leverage their capabilities [13, 14, 32, 36, 47]. In light of the difficulties associated with obtaining ground truth images for fully supervised learning methods [16, 23, 31], we explored the feasibility of single-point weak supervision for SSTD tasks. Recent advances in single-point weak supervision in computer vision [20, 24, 49] have highlighted its potential to significantly reduce annotation efforts. Building on these insights and to address the next two challenges, this work pioneers the application of a single-point weakly supervised strategy for SSTD. Specifically, we propose the teacher-student framework for pseudo-label evolution, which first utilizes the zero-shot capabilities of SAM to generate initial pseudo-labels from point annotations. The teacher model is fine-tuned through low-rank adaptation with the filtered pseudo-labels and can segment more weak texture stripes. The refined pseudo-labels are also employed to train the student model, StripeNet, to distill knowledge from the teacher model and enlarge the search space for better pseudo-labels. This iterative teacher-student mechanism facilitates the evolution of pseudo-label and improves the accuracy of SSTD. Our contributions in this work are manifold, outlined as follows:

- The AstroStripeSet dataset was introduced as a pioneering resource for SSTD research, featuring synthesized images under diverse stray light conditions.
- The development of a novel teacher-student framework for single-point weakly supervised training, significantly enhances the quality of pseudo-labels.
- The proposal of a new loss function, GeoDice, informed by the linear-like shape characteristics of stripe-like space targets.
- Extensive experimental validation demonstrates that our framework achieves SOTA performance, comparable to fully supervised methods across various metrics.

The structure of this paper is organised into several sections. Section 2 presents the related work. Section 3 details the AstroStripeSet dataset. Section 4 elaborates on our teacher-student single-point supervision. Section 5 presents experimental validation of our approach. Section 6 concludes our findings.

2 Related Work

This section explores existing methodologies and highlights the evolution of detection techniques in complex backgrounds, categorizing them into geometric feature-based, pattern-based, and data-driven approaches.

2.1 Geometric Feature-Based Approaches

Geometric feature-based methods leverage the accumulation of information in parameter spaces or integral transformations to detect stripe targets in images. These approaches, often employing the Hough or Radon transforms, gradually refine detection through iterative processes. Hickson et al. [11] combined matched filtering with an improved Radon transform for stripe detection. Jiang et al. [17, 18] utilized enhanced median filtering and Hough transform methods for extracting stripe-like targets against non-uniform backgrounds. Liu et al. [28] and Xi et al. [44] applied time-index filtering methods to remove stars and noise, subsequently detecting stripes through multi-frame state transfer and multi-stage hypothesis testing. Despite achieving notable results in specific scenarios, these methods face limitations in handling background clutter, noise, and the variable scales of targets, which are determined by the inherent properties of the Hough and Radon transforms.

2.2 Pattern-Based Approaches

Pattern-based approaches, akin to geometric feature-based methods, commence with filtering algorithms to mitigate space stray light and stars. The distinction lies in their extraction techniques, where multiple stripe-matching templates of different orientations are designed to detect stripe-like targets. Virtanen et al. [42] introduced a multi-window geometric feature analysis for automatic stripe-like target detection, requiring motion prior information. Dawson et al. [5] and Sara et al. [38] explored stripe pattern matching filters and weak stripe detection methods based on stripe pattern distribution, respectively. A recent work by Lin et al. [26] attempted to detect stripe patterns through pattern clustering. However, these methods struggle under strong stray light interference and fail to detect weakly manifested or morphologically distinct stripe-like targets.

2.3 Data-Driven Approaches

The integration of convolutional neural networks (CNN) into SSTD signifies a shift towards data-driven methods, focusing on automatic learning of stripe features from extensively labeled images. Jia et al. [16] utilized the fast RCNN

network for classifying astronomical targets, including point stars and stripe-like space targets. Li et al. [23] and Liu et al. [31] adopted hierarchical network structures based on U-Net to address stray light interference, providing valuable insights for the field. Tao et al. [41] proposed SDebrisNet, a stripe detection network leveraging CNN and attention mechanisms, though its efficacy under intense stray light remains unreported. The variability of stray light and stripe-like targets prevents the universal target detector YOLO [34, 35] and RCNN [8, 10] series networks from achieving optimal results. In addition, there are some advanced networks for complex contexts, such as ISNet [53], ACM [3], DNANet [21], APGCNet [54], RDIAN [40], but they all rely on pixel-level annotation. Geometric and pattern-based approaches have laid the groundwork for SSTD, and the advent of data-driven methods promises enhanced detection capabilities. However, the field continues to grapple with the challenges of dataset availability, annotation costs, and model adaptability to the unique conditions of space imaging. The exploration of weakly supervised learning and the potential of foundation models in this domain represent promising avenues for overcoming these hurdles.

3 AstroStripeSet Dataset

The scarcity of open-source datasets poses a critical bottleneck for SSTD research. To address this gap, our work introduces AstroStripeSet, a pioneering dataset that stands as the first comprehensive public disclosure in this specialized field. Notably, AstroStripeSet eclipses the scale of previously known datasets, both in terms of volume and background diversity, making it the largest and open-source dataset of its kind available to the research community. Due to the high cost of obtaining a large number of real space images just for academic research purposes, this is the main reason why there has been no large open source dataset in the field of SSTD. Thus, AstroStripeSet has been synthesized to emulate the complex space scenes. It encompasses a diverse array of space stray lights and sensor disturbances, including reflections from the earth, moon, and sun, cosmic rays, and stellar background interference. Furthermore, the dataset features stripe-like targets with diverse positions, scales, orientations, and brightness distributions, thereby offering a rich dataset for the development and testing of SSTD methodologies. Unique to AstroStripeSet is the provision of three distinct forms of annotations: single-point annotation, precise pixel-level annotation, and bounding box annotation, catering to a wide range of research needs from basic detection algorithms to complex segmentation and localization tasks. The dataset comprises 1500 combinations of raw images and their corresponding labeled images.

Table 1 shows a comparative analysis with existing datasets, revealing the unparalleled advantages of AstroStripeSet. It significantly exceeds the volume of datasets provided by predecessors, facilitating a more robust and comprehensive approach to model training and testing. The diversity introduced by AstroStripeSet, encompassing various space stray lights, sensor noises, and dis-

Table 1: Comparison with existing space target datasets

Dataset	Volume	Diversity	Category	Annotation	Open/Private
Lin et al. [26]	83	One	Stripe	None	Private
Jiang et al. [18]	200	One	Stripe	None	Private
Liu et al. [30]	111	One	Point	None	Private
Yao et al. [48]	100	Two	Point	None	Private
Francesco et al. [7]	400	One	Point	None	Private
Ours	1500	Four	Stripe	Three	Open

turbances, is crucial for the development of models capable of generalizing across a wide range of real-world scenarios. Focused on stripe-like targets, the dataset fills a specific niche in SSTD research, offering a dedicated resource for exploring stripe detection in space images. Moreover, the multi-faceted annotation approach and the dataset’s open accessibility promote transparency, reproducibility, and collaborative advancements in the field. This dataset is poised to catalyze significant progress in detecting and analyzing stripe-like space targets, offering a valuable resource for developing more accurate and robust detection systems.

4 Teacher-Student Single-point Supervision

The teacher-student framework is depicted in Figure 2. The initial pseudo labels are generated from an off-shelf pre-trained SAM, and then the labels iteratively evolve between teacher and student networks from initial pseudo labels to more accurate stripe-like space target detection. This framework integrates two core components: the StripeSAM, a low-rank adaptation fine-tuned that functions as the teacher network, and the novel StripeNet, which serves as the student network. Together, these elements facilitate the progressive refinement of pseudo labels. Traditional dice loss, while effective, lacks the directional sensitivity crucial for segmenting linearly oriented targets. To address this, a customized GeoDice loss function is introduced for StripeNet, enhancing its ability to discern and segment weakly textured stripe-like space targets. This innovative loss function leverages the inherent straight-line-like prior information of striped targets, significantly bolstering the segmentation capabilities of both StripeSAM and StripeNet through their collaborative iterative evolution.

4.1 Initial Pseudo Labels from Pre-trained SAM

The foundational step in our teacher-student framework for stripe-like space target detection involves generating initial pseudo labels using the pre-trained SAM. This process begins with feeding the space images, containing the stripe-like target, into the image encoder for generating image embeddings. Concurrently, annotated target point labels serve as point prompts for the striped target area, and are input into the prompt encoder for prompt embeddings. The mask encoder will generate pseudo-labels by mapping image and prompt embeddings

to the output token. To be specific, input for the pre-trained SAM includes images \mathcal{X} , and point prompts, \mathcal{P} , i.e. $\mathcal{X} = \{\mathbf{x}_i | i \in \{1, 2, \dots, N\}, \mathbf{x}_i \subseteq \mathbb{R}^d\}$, and $\mathcal{P} = \{(u_i, v_i) | i \in \{1, 2, \dots, N\}\}$, (u_i, v_i) is the single-point annotation for each image.

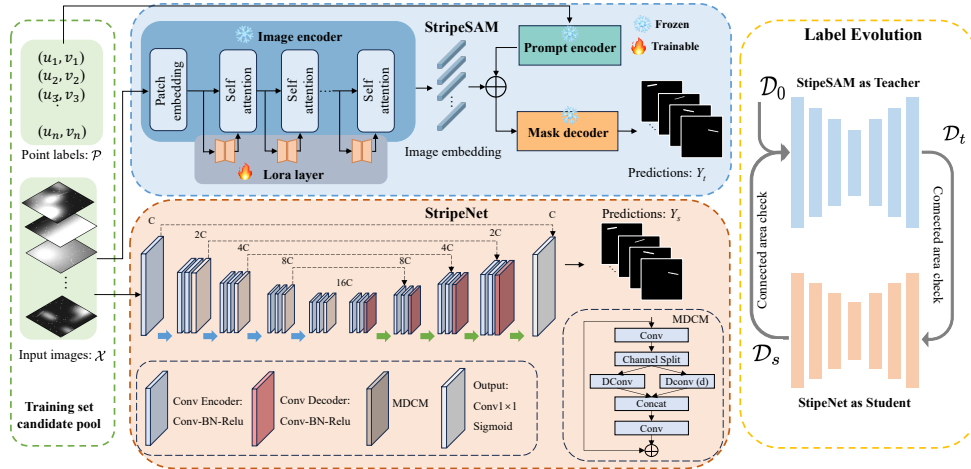


Fig. 2: An overall framework for label evolution under a single point of weak supervision.

The pre-trained SAM is trained for general segmentation tasks rather than space-target segmentation, so the output tends to be very noisy. To overcome this limitation, we take advantage of the prior knowledge that there is only one object in each image of the AstroStripeSet dataset, and the outputs with more than one object are treated as false positives and filtered out. We count the number of objects by detecting the connected area, and each connected area is one object. The filtering process is called ‘connected area check’. After that, the remaining segmentation masks are kept as the initial pseudo-labels, $\mathcal{Y}_0 = \{\mathbf{y}_i | i \in \{1, 2, \dots, N_0\}, \mathbf{y}_i \subseteq \mathbb{R}^d\}$, \mathbf{y}_i is the segment map and has the same size as the input image \mathbf{x}_i , the number of the selected images N_0 is usually much less than the number of input image N . The inference is shown as Equation 1, in which the $\mathcal{F}(\cdot)$ is ‘connected area check’ and $\mathcal{H}(\cdot)$ is the pre-trained SAM.

$$\mathcal{Y}_0 = \{\mathcal{F}(\mathcal{H}(\mathbf{x}_i, u_i, v_i)) | \mathbf{x}_i \in \mathcal{X}, (u_i, v_i) \in \mathcal{P}, i \in \{1, 2, \dots, N\}\} \quad (1)$$

With the input image, point prompt, and pseudo labels, we can construct our initial training dataset, $\mathcal{D}_0 = (\mathcal{X}_0, \mathcal{P}_0, \mathcal{Y}_0) = \{(\mathbf{x}_i, (u_i, v_i), \mathbf{y}_i)\}_{1}^{N_0}$, which will be sent to the subsequent modules to start the loop of label evolution.

4.2 StripeSAM with Lora Fine-tuning as the Teacher

Despite its proficiency in zero-shot segmentation within high SNR scenarios, the pre-trained SAM has very limited capability in segmenting striped images under

conditions of intense stray light, the deficiency of which may be caused by the absence of noisy training samples and the lack of prior knowledge concerning stripe patterns amidst stray light. To address this issue, we fine-tune the SAM model with the selected dataset. The dataset selection is achieved with prior human knowledge about stripe-like space targets, in other words, we are using the human prior knowledge to automatically distill knowledge from the foundation model, SAM. The low-rank adaption (LoRA) [12] is applied to fine-tune the SAM model, in which a novel low-rank weight matrix within the image encoder is incorporated, as shown in the Figure 2. The SAM can be retrained efficiently by updating only a minimal subset of parameters. The fine-tuned SAM, referred to hereafter as StripeSAM, serves as the teacher network in the label evolution framework. The original weight parameters of StripeSAM are frozen and the low-rank matrices are trained with selected pseudo-labels with some segmentation maps under conditions of intense stray lights. By doing this, we find that StripeSAM not only demonstrates superior label quality over the pre-trained SAM but also enriches the dataset with additional pairs of weakly labeled data. After StripeSAM is fine-tuned, we use the StripeSAM $\mathcal{G}(\cdot)$ to infer all images to generate the new pseudo-labels, as shown in Equation 2. These labels go through the ‘connected area check’ again to filter out noisy labels, and the remained pseudo-labels \mathcal{Y}_t and their mass center points of target area \mathcal{P}_t are used to train the following student network. Up to here, we obtain our new training dataset, $\mathcal{D}_t = (\mathcal{X}_t, \mathcal{P}_t, \mathcal{Y}_t) = \{(\mathbf{x}_i, (u_i, v_i), \mathbf{y}_i)\}_1^{N_t}$.

$$\mathcal{Y}_t = \{\mathcal{F}(\mathcal{G}(\mathbf{x}_i, u_i, v_i)) | \mathbf{x}_i \in \mathcal{X}_0, (u_i, v_i) \in \mathcal{P}_0, i \in \{1, 2, \dots, N_0\}\} \quad (2)$$

4.3 StripeNet with Multiscale Feature Fusion as the Student

To leverage the enhanced stripe pattern recognition capabilities of the teacher network StripeSAM, we introduce StripeNet, a student network characterized by a streamlined encoder-decoder architecture, as shown in Figure 1. The encoder phase consists of many multi-scale dilated convolution modules (MDCM) and is aimed at heightening the network’s sensitivity to striped targets across varying scales. The introduction of StripeNet not only refines the quality of labeling but also enlarges the repository of data pairs with weak masks. The dataset \mathcal{D}_t from the teacher network is used to train this student network, after that, the model is used to infer the pseudo-labels for the next iteration. The label inference is as Equation 3, in which $\mathcal{E}(\cdot)$ represents the StripeNet.

$$\mathcal{Y}_s = \{\mathcal{F}(\mathcal{E}(\mathbf{x}_i, u_i, v_i)) | \mathbf{x}_i \in \mathcal{X}_t, (u_i, v_i) \in \mathcal{P}_t, i \in \{1, 2, \dots, N_t\}\} \quad (3)$$

The point prompts are required to train the StripeSAM, and we calculate the mass central point of the detected area in each segmentation map for point prompts \mathcal{P}_s . Therefore, we can construct a new dataset, $\mathcal{D}_s = (\mathcal{X}_s, \mathcal{P}_s, \mathcal{Y}_s) = \{(\mathbf{x}_i, (u_i, v_i), \mathbf{y}_i)\}_1^{N_s}$. This enriched dataset is then cycled back to StripeSAM. Our label change process is initialized from pre-training SAM with single-point labels, and then iteratively loops in the teacher-student framework, which is called the label evolution. We find that more and more pseudo-labels under conditions of intensive stray light will be exploited as the label evolution starts.

4.4 Label Evolution and GeoDice Loss Function

It is well observed that stripe-like space targets are usually similar to straight lines, based on which we propose a new loss function, called GeoDice Loss. As shown in Equation 5, it consists of geometric alignment loss \mathcal{L}_g and weighted dice loss \mathcal{L}_d . The GeoDice loss is designed to make segmentation results closer to real straight-line stripes by incorporating the geometric direction information, therefore, resulting in better target segmentation. To implement this loss, we first divide the binary prediction map into connected regions and then calculate the longest straight line in each connected region. To ensure the simplicity of straight determination, we use the farthest point sampling algorithm to determine the two endpoints of the longest straight line from each connected area in the prediction map and the ground truth (GT). Then, the angle difference of the straight line between GT and prediction is calculated and multiplied by the Sigmoid output of the predicted image to ensure its differentiability, and angle differences are averaged as L_g . The specific calculation formula of L_g is as follows:

$$\mathcal{L}_g = \frac{1}{N} \sum_{i=1}^N \left(\eta \left(\frac{\sum_{j=1}^{M_i} \min(\angle(p_j, g_i), \pi - \angle(p_j, g_i)) \times \sigma(p_j)}{M_i} \right) \right) \quad (4)$$

where N is the number of images in the batch, and M_i is the number of connected regions of the i -th image, $\sigma(\cdot)$ is the sigmoid function, $\eta(\cdot)$ is the normalization function, $\angle(p_j, g_i)$ represents the angle difference between the j -th connected predicted area p_j and ground truth g_i . Finally, our final GeoDice can be expressed the Equation 5, in which α and λ are the weighting value.

$$\mathcal{L}_{Geo} = \alpha \times \mathcal{L}_g + \lambda \times \mathcal{L}_d \quad (5)$$

5 Results and Experiments

5.1 Experimental Setup

This subsection provides an overview of the components critical to our experimental framework. It briefly describes the dataset, evaluation metrics, and training parameters, along with implementation details.

Dataset: In response to the inaccessibility of a large public data set designed for SSTD using deep learning approaches, we have used an in-house dataset described in Section 3. To thoroughly evaluate the efficacy of our proposed method under a variety of stray light conditions, the test set has been divided into four distinct subsets. Each subset corresponds to a unique type of stray light, namely sunlight, moonlight, earthlight, and interstellar mixed light. Comprising 100 images each, these subsets present complex backgrounds that challenge the method's ability to accurately detect stripe-like targets. This structured approach enhances our analysis, allowing for a detailed assessment of the method's adaptability and performance in the face of different stray light conditions.

Evaluation Metrics: To quantitatively assess our proposed method, we use key evaluation metrics including Mean Intersection over Union (mIoU) [4] and

Table 2: Comparison with different SOTA networks.

Type	Method	Sun Light			Moon Light			Earth Light			Mixed Light		
		Dice	mIoU	P _d	F _a	Dice	mIoU	P _d	F _a	Dice	mIoU	P _d	F _a
Zero	SAM-b	25.85	22.05	26.0	54.07	42.61	37.81	46.0	45.53	38.96	34.55	42.0	38.44
	SAM-l	35.49	31.20	37.0	48.85	51.26	46.20	54.0	37.76	44.76	39.67	46.0	30.19
	SAM-h	42.42	37.02	44.0	30.15	56.23	50.37	60.0	28.77	53.16	46.96	57.0	21.67
Full	UNet	90.60	83.75	97.0	0.10	89.15	82.76	95.0	0.10	90.04	84.01	95.0	0.09
	ACM	81.70	72.49	90.0	0.16	80.99	72.90	88.0	0.15	81.59	73.0	89.0	0.15
	DNA Net	89.85	82.16	98.0	0.11	88.93	80.44	94.0	0.11	89.51	81.48	96.0	0.11
	RDIAN	87.34	78.89	93.0	0.13	86.91	78.82	94.0	0.12	88.29	80.45	95.0	0.12
	AGPCNet	86.83	78.43	94.0	0.13	86.67	78.44	95.0	0.12	88.39	80.33	94.0	0.12
	MResUnet	26.51	21.42	23.0	0.43	40.46	34.12	40.0	0.33	38.31	32.69	38.0	0.37
	UCTransNet	91.11	84.38	98.0	0.01	91.46	85.21	99.0	0.008	91.52	85.24	98.0	0.009
	StripeNet	92.81	86.99	100.0	0.07	90.57	85.16	97.0	0.07	90.89	85.24	96.0	0.08
	StripeSAM	84.47	74.52	92.0	0.16	84.74	75.23	91.0	0.14	84.40	75.31	92.0	0.16
Weak	StripeNet	85.50	75.44	96.0	0.002	85.93	76.35	97.0	0.002	86.95	77.81	97.0	0.003
	StripeSAM												

Dice coefficient [6] for pixel-level accuracy, along with Probability of Detection (P_d) and false alarm rate (F_a) for target-level performance. The IoU metric measures the overlap between the predicted and actual images, while the Dice coefficient evaluates their similarity, with values closer to 1 indicating higher accuracy. These metrics are particularly effective in assessing the algorithm's segmentation precision in identifying details within the target area. Furthermore, P_d quantifies the algorithm's success in correctly identifying stripe-like targets, and F_a calculates the rate of incorrect detections, providing insight into the algorithm's sensitivity and specificity in distinguishing true targets from false alarms. In particular, images are considered successfully detected with an IoU value greater than 50%, while pixels outside the target region are classified as false alarms. Together, these metrics offer a comprehensive evaluation of the algorithm's performance in detecting stripe-like targets with precision and minimizing false positives.

Computational Setup and Training Configuration: The experimental evaluations were conducted using an RTX 4080 GPU, with PyTorch version 2.2.0 and CUDA 12.1. StripeSAM is trained over 50 epochs with an initial learning rate of 0.0001 and a batch size of 1. On the contrary, StripeNet undergoes 350 training epochs with a starting learning rate of 0.01 and a batch size of 4. Throughout the training phase, a cosine annealing strategy was employed to dynamically adjust the learning rate. Optimization of the network training process was achieved through the use of the Adam optimizer, known for its effectiveness in converging towards optimal solutions.

5.2 Results and Discussion

A comprehensive analysis of the outcomes of our proposed approach is discussed in this section. It begins with a detailed examination of the quantitative results, where comparisons are drawn between our approach and SOTA across various stray-light conditions. Following quantitative analysis, a qualitative evaluation is presented, offering visual evidence of the effectiveness of our method, particularly in stripe detection under challenging environmental conditions.

Input	GT	StripeSAM	StripeNet	ACM	DNA Net	APGCNet	RDIAN	UCTransNet	MResUnet	UNet	SAM-b

Fig. 3: Visual comparison of our method with the SOTA fully supervised network on the upcoming AstroStripeSet. (True targets, misses, and false alarms are highlighted in red, blue, and yellow, respectively).

Quantitative Results: Traditional methods based on geometric [17, 18, 28] and pattern [5, 26, 38] information struggle in scenarios with variable and intense stray light, making them unsuitable for direct comparison. Consequently, our evaluation primarily targets SOTA fully supervised deep learning models, such as UNet [37], ACM [3], DNANet [21], AGPCNet [54], RDIAN [40], MResUnet [15], and UCTransNet [43]. Furthermore, we compare our method with three pre-trained SAMs [19] employing single point prompts, denoted SAM-b, SAM-l and SAM-h. Table 2 presents a comprehensive quantitative comparison between the proposed methodology and existing SOTA techniques. The analysis reveals that the performance of our teacher-student network significantly surpasses that of pre-trained single-point prompt SAM models across all four categories of challenging test images. This enhancement is not only in terms of segmentation accuracy but also in the substantial reduction of manual annotation time, achieving a performance level on par with fully supervised network methods. Such advancements are attributed to the innovative implementation of a new label evolution network and the introduction of a customized GeoDice loss function, which collectively contribute to the superior performance of our approach. The table further illustrates the varied performance of different SOTA methods under each stray light condition, providing a nuanced view of their respective strengths and limitations. For example, UCTransNet exhibits remarkable performance across all stray light scenarios, highlighting its robustness and adaptability. In contrast, the performance of MResUnet significantly lags, particularly under challenging stray light conditions, underscoring the importance of methodological innovation in addressing the complexities of image segmentation.

Qualitative Assessment: This section examines the adeptness of our proposed StripeSAM method to show the detection of targets within environments characterized by low SNR. This is elucidated through a visual comparison, as shown in Figure 3, comparing our approach against SOTA networks in eight images, each depicting space stripe targets under a variety of stray light conditions. The pre-trained SAM basically loses its ability to segment stripe-like targets under low SNR. While RDIAN is capable of detecting targets in low SNR, it tends to produce a high number of false alarms. StripeSAM exhibits a commendable performance, on par with that of fully supervised UCTransNet, particularly in retaining the intricacies of stripe details throughout the spectrum of challenging images. The proficiency of StripeSAM is evident, as it consistently identifies true targets (marked in red), minimizes misses (marked in blue), and avoids false alarms (marked in yellow) with notable accuracy. Therefore, our findings substantiate the potential of StripeSAM as a superior alternative to the fully supervised SOTA methods in the context of stripe-like target detection amidst low SNR.

Table 3: The impact of different ranks in StripeSAM

Rank	Sun Light				Moon Light				Earth Light				Mixed Light			
	Dice	mIoU	P _d	F _a	Dice	mIoU	P _d	F _a	Dice	mIoU	P _d	F _a	Dice	mIoU	P _d	F _a
1	42.98	37.62	47.0	0.64	51.39	45.57	53.0	0.52	59.87	53.15	65.0	0.74	45.73	40.51	47.0	0.93
8	56.80	49.07	58.0	1.54	65.93	58.32	69.0	1.13	68.42	60.87	74.0	0.79	58.12	50.27	54.0	1.61
32	56.01	48.69	57.0	1.27	63.96	56.75	66.0	1.14	67.88	60.49	75.0	1.44	57.59	50.40	58.0	1.41
128	59.85	51.67	62.0	1.02	67.20	59.26	70.0	0.69	67.75	60.48	74.0	0.99	62.14	53.82	62.0	1.08
512	61.68	53.35	63.0	0.41	70.52	62.76	75.0	0.03	67.91	60.56	74.0	0.27	61.49	53.62	61.0	0.53
1024	61.92	53.44	64.0	0.82	67.48	59.84	73.0	1.32	68.92	61.27	75.0	0.56	62.46	53.86	62.0	0.48

5.3 Ablation Study

In this Section our investigation into the StripeSAM entailed tuning the rank parameter, which is crucial to modify the additionally introduced trainable weight parameters effectively. We compared various loss functions to determine their effectiveness with StripeNet, identified the optimal iteration count for the teacher-student network, and evaluated the model’s zero-shot capability for testing generalization.

Evaluating Rank Parameter: The rank parameter within LoRA-based architectures, such as StripeSAM, plays a pivotal role in modulating the trade-off between computational efficiency and the effectiveness of adapting pre-trained models for novel tasks. Essentially, a higher rank correlates with an increased number of trainable parameters, thereby influencing the model’s adaptability and performance. To elucidate the effect of varying rank values on StripeSAM, we refer to the results of the first iteration in Table 3. It indicates that a rank setting of 512 yields the most balanced and superior performance across all four evaluated datasets. Consequently, this rank value of 512 is adopted within our teacher-student network framework to optimize the balance between efficiency and task-specific adaptation effectiveness.

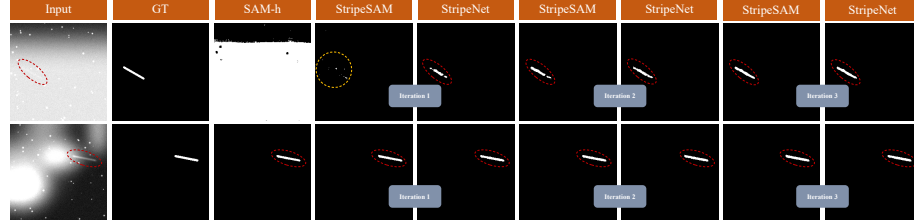
Table 4: Comparison results of different loss functions in StripeNet

Loss	Sun Light				Moon Light				Earth Light				Mixed Light			
	Dice	mIoU	P _d	F _a	Dice	mIoU	P _d	F _a	Dice	mIoU	P _d	F _a	Dice	mIoU	P _d	F _a
SoftIoU	68.73	55.24	68.0	0.40	70.45	57.22	68.0	0.36	72.39	59.68	75.0	0.35	68.53	56.79	71.0	0.38
Wdice	75.98	66.54	78.0	0.20	76.60	67.90	78.0	0.18	77.65	68.89	83.0	0.20	72.89	64.73	73.0	0.25
WDice+Focal	76.85	67.19	81.0	0.21	78.56	69.63	84.0	0.17	80.16	70.60	85.0	0.19	73.98	64.99	79.0	0.24
SoftIoU+Focal	72.99	64.67	79.0	0.21	76.19	68.09	83.0	0.18	78.91	70.36	84.0	0.19	73.10	65.06	79.0	0.24
GeoDice	82.05	71.76	89.0	0.18	81.42	72.04	88.0	0.16	80.56	71.24	87.0	0.19	73.44	64.64	78.0	0.24

Table 5: The impact of different iterations of teacher-student on detection results

Iteration	Method	Sun Light				Moon Light				Earth Light				Mixed Light			
		Dice	mIoU	P _d	F _a	Dice	mIoU	P _d	F _a	Dice	mIoU	P _d	F _a	Dice	mIoU	P _d	F _a
1	StripeSAM	61.67	53.35	63.0	0.41	70.52	62.76	75.0	0.03	67.91	60.55	74.0	0.27	61.49	53.62	61.0	0.53
	StripeNet	75.08	65.40	79.0	0.21	75.62	67.44	78.0	0.18	77.47	68.44	83.0	0.19	71.45	62.69	71.0	0.25
2	StripeSAM	82.04	71.58	88.0	0.004	84.27	74.76	91.0	0.006	84.75	75.43	89.0	0.008	81.85	71.96	85.0	0.01
	StripeNet	77.71	68.41	81.0	0.19	81.02	71.68	86.0	0.16	82.51	73.43	89.0	0.16	77.36	68.58	82.0	0.22
3	StripeSAM	85.45	75.44	96.0	0.001	85.93	76.35	97.0	0.001	86.94	77.81	97.0	0.003	85.28	75.75	93.0	0.01
	StripeNet	84.47	75.52	92.0	0.16	84.74	75.23	91.0	0.15	84.40	75.31	92.0	0.16	81.18	71.72	84.0	0.20

Comparative Analysis of Loss Functions: Table 4 shows the results of different loss functions for the first iteration of StripeNet. The loss functions used for comparative analysis primarily include traditional segmentation loss functions and their ensembles, such as weighted dice loss [22] and softIoU loss [21]. Each loss function is paired with focal loss [27] in an equal weight ratio of 1: 1. The quantitative results demonstrate that our customized GeoDice loss function effectively leverages straight-line prior information, significantly improving the detection rate of stripe-like space targets while ensuring segmentation accuracy.

**Fig. 4:** Visual results from three iterations in the label evolution process.(True targets and false alarms are highlighted in red and yellow, respectively).

Iterative Label Evolution : As noted previously, the pre-trained SAM can produce excellent results when the target is spotted without the noise. However, it struggles with segmentation of stripe-like targets under challenging conditions characterized by a low signal-to-noise ratio. It can be seen in Figure 4 and Table 5 that our proposed iterative approach improves the segmentation of the stripe-like targets. Table 5 presents the quantitative segmentation performance of StripeSAM and StripeNet for various iteration numbers, further demonstrating the effectiveness of our label evolution framework.

Zero-Shot Generalization: This section delves into the generalizability and transferability of our model, particularly in contexts beyond the confines of our dataset, and benchmarks its performance against other methodologies. Figure 5 offers a comparative analysis of the detection results of various approaches with space stray light conditions of the real world. In particular, StripeSAM and StripeNet exhibit a pronounced ability to accurately identify stripe-like targets while minimizing false positives, surpassing the performance of other fully supervised SOTA networks. This demonstration of effective zero-shot generalization not only underscores the robust adaptability of our networks but also corroborates the value of our specially curated AstroStripeSet dataset in preparing the network for real-world challenges.

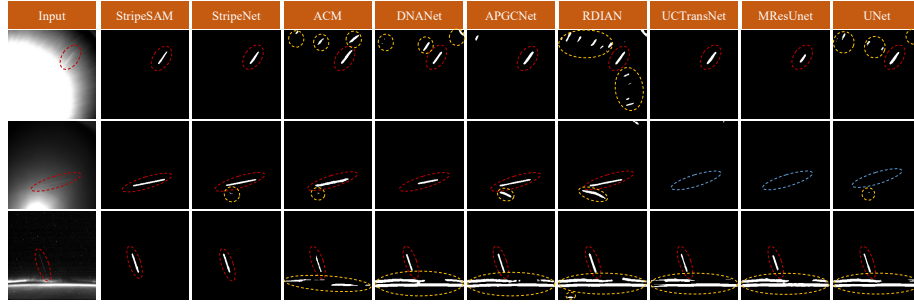


Fig. 5: Visual comparison of detection under real stray light background in space orbit. (True targets, misses, and false alarms are highlighted in red, blue, and yellow, respectively).

6 Conclusion

In this study, we introduce AstroStripeSet, the inaugural dataset destined for open-source release in the Stripe-like Space Target Detection (SSTD) domain, establishing a new benchmark for future evaluations. We also present an innovative label evolution teacher-student model, employing single-point supervision alongside a custom GeoDice loss function, specifically designed for the identification of stripe-like targets under complex stray light conditions. Our comprehensive experiments demonstrate the method’s exceptional performance in SSTD, offering a novel perspective and expanding the scope of research in weakly supervised methods within this field. Looking ahead, our goal is to explore the adaptation of our methodology to other segmentation challenges, incorporate other semi-supervised and unsupervised learning techniques, and investigate dynamic loss function adaptation and cross-domain transfer learning to enhance model versatility and applicability. Collecting more challenging real-space background images will also be a priority, further propelling SSTD research.

References

1. Caron, M., Touvron, H., Misra, I., Jégou, H., Mairal, J., Bojanowski, P., Joulin, A.: Emerging properties in self-supervised vision transformers. In: Proceedings of the IEEE/CVF international conference on computer vision. pp. 9650–9660 (2021) 3
2. Chen, W.C., Jan, S.S.: Star tracking algorithm based on local dynamic background reduction for eliminating stray light interference from star spot data. *IEEE Sensors Journal* (2023) 2
3. Dai, Y., Wu, Y., Zhou, F., Barnard, K.: Asymmetric contextual modulation for infrared small target detection. In: Proceedings of the IEEE/CVF Winter Conference on Applications of Computer Vision. pp. 950–959 (2021) 5, 11
4. Dan, B., Zhu, Z., Qi, X., Zhang, J., Ouyang, Y., Li, M., Tang, T.: Dynamic weight guided smooth-sparse decomposition for small target detection against strong vignetting background. *IEEE Transactions on Instrumentation and Measurement* (2023) 2, 9
5. Dawson, W.A., Schneider, M.D., Kamath, C.: Blind detection of ultra-faint streaks with a maximum likelihood method. *arXiv preprint arXiv:1609.07158* (2016) 4, 11
6. Deng, R., Shen, C., Liu, S., Wang, H., Liu, X.: Learning to predict crisp boundaries. In: Proceedings of the European conference on computer vision (ECCV). pp. 562–578 (2018) 10
7. Diprima, F., Santoni, F., Piergentili, F., Fortunato, V., Abbattista, C., Amoruso, L.: Efficient and automatic image reduction framework for space debris detection based on gpu technology. *Acta Astronautica* **145**, 332–341 (2018) 2, 6
8. Faster, R.: Towards real-time object detection with region proposal networks. *Advances in neural information processing systems* **9199**(10.5555), 2969239–2969250 (2015) 5
9. Guo, L., Zhang, W., Wang, Z., Sun, X., Shang, Y.: Weak geo satellite target detection based on image transformation and energy accumulation. In: Proceedings of the 2021 4th International Conference on Image and Graphics Processing. pp. 52–58 (2021) 2
10. He, K., Gkioxari, G., Dollár, P., Girshick, R.: Mask r-cnn. In: Proceedings of the IEEE international conference on computer vision. pp. 2961–2969 (2017) 5
11. Hickson, P.: A fast algorithm for the detection of faint orbital debris tracks in optical images. *Advances in Space Research* **62**(11), 3078–3085 (2018) 4
12. Hu, E.J., Shen, Y., Wallis, P., Allen-Zhu, Z., Li, Y., Wang, S., Wang, L., Chen, W.: Lora: Low-rank adaptation of large language models. *arXiv preprint arXiv:2106.09685* (2021) 8
13. Hu, M., Li, Y., Yang, X.: Skinsam: Empowering skin cancer segmentation with segment anything model. *arXiv preprint arXiv:2304.13973* (2023) 3
14. Huang, Y., Yang, X., Liu, L., Zhou, H., Chang, A., Zhou, X., Chen, R., Yu, J., Chen, J., Chen, C., et al.: Segment anything model for medical images? *Medical Image Analysis* p. 103061 (2023) 3
15. Ibtehaz, N., Rahman, M.S.: Multiresunet: Rethinking the u-net architecture for multimodal biomedical image segmentation. *Neural networks* **121**, 74–87 (2020) 11
16. Jia, P., Liu, Q., Sun, Y.: Detection and classification of astronomical targets with deep neural networks in wide-field small aperture telescopes. *The Astronomical Journal* **159**(5), 212 (2020) 3, 4

17. Jiang, P., Liu, C., Yang, W., Kang, Z., Fan, C., Li, Z.: Space debris automation detection and extraction based on a wide-field surveillance system. *The Astrophysical Journal Supplement Series* **259**(1), 4 (2022) [4](#), [11](#)
18. Jiang, P., Liu, C., Yang, W., Kang, Z., Li, Z.: Automatic space debris extraction channel based on large field of view photoelectric detection system. *Publications of the Astronomical Society of the Pacific* **134**(1032), 024503 (2022) [4](#), [6](#), [11](#)
19. Kirillov, A., Mintun, E., Ravi, N., Mao, H., Rolland, C., Gustafson, L., Xiao, T., Whitehead, S., Berg, A.C., Lo, W.Y., et al.: Segment anything. arXiv preprint arXiv:2304.02643 (2023) [3](#), [11](#)
20. Li, B., Wang, Y., Wang, L., Zhang, F., Liu, T., Lin, Z., An, W., Guo, Y.: Monte carlo linear clustering with single-point supervision is enough for infrared small target detection. In: *Proceedings of the IEEE/CVF International Conference on Computer Vision (ICCV)*. pp. 1009–1019 (October 2023) [3](#)
21. Li, B., Xiao, C., Wang, L., Wang, Y., Lin, Z., Li, M., An, W., Guo, Y.: Dense nested attention network for infrared small target detection. *IEEE Transactions on Image Processing* **32**, 1745–1758 (2022) [5](#), [11](#), [13](#)
22. Li, X., He, M., Li, H., Shen, H.: A combined loss-based multiscale fully convolutional network for high-resolution remote sensing image change detection. *IEEE Geoscience and Remote Sensing Letters* **19**, 1–5 (2021) [13](#)
23. Li, Y., Niu, Z., Sun, Q., Xiao, H., Li, H.: Bsc-net: Background suppression algorithm for stray lights in star images. *Remote Sensing* **14**(19), 4852 (2022) [3](#), [5](#)
24. Li, Y., Zhao, H., Qi, X., Chen, Y., Qi, L., Wang, L., Li, Z., Sun, J., Jia, J.: Fully convolutional networks for panoptic segmentation with point-based supervision. *IEEE Transactions on Pattern Analysis and Machine Intelligence* **45**(4), 4552–4568 (2022) [3](#)
25. Lin, B., Yang, X., Wang, J., Wang, Y., Wang, K., Zhang, X.: A robust space target detection algorithm based on target characteristics. *IEEE Geoscience and Remote Sensing Letters* **19**, 1–5 (2021) [2](#)
26. Lin, B., Zhong, L., Zhuge, S., Yang, X., Yang, Y., Wang, K., Zhang, X.: A new pattern for detection of streak-like space target from single optical images. *IEEE Transactions on Geoscience and Remote Sensing* **60**, 1–13 (2021) [2](#), [4](#), [6](#), [11](#)
27. Lin, T.Y., Goyal, P., Girshick, R., He, K., Dollár, P.: Focal loss for dense object detection. In: *Proceedings of the IEEE international conference on computer vision*. pp. 2980–2988 (2017) [13](#)
28. Liu, D., Wang, X., Xu, Z., Li, Y., Liu, W.: Space target extraction and detection for wide-field surveillance. *Astronomy and Computing* **32**, 100408 (2020) [2](#), [4](#), [11](#)
29. Liu, D., Wang, X., Li, Y., Xu, Z., Wang, J., Mao, Z.: Space target detection in optical image sequences for wide-field surveillance. *International Journal of Remote Sensing* **41**(20), 7846–7867 (2020) [2](#)
30. Liu, D., Chen, B., Chin, T.J., Rutten, M.G.: Topological sweep for multi-target detection of geostationary space objects. *IEEE Transactions on Signal Processing* **68**, 5166–5177 (2020) [2](#), [6](#)
31. Liu, L., Niu, Z., Li, Y., Sun, Q.: Multi-level convolutional network for ground-based star image enhancement. *Remote Sensing* **15**(13), 3292 (2023) [3](#), [5](#)
32. Ma, J., Wang, B.: Segment anything in medical images. arXiv preprint arXiv:2304.12306 (2023) [3](#)
33. Oquab, M., Dariseti, T., Moutakanni, T., Vo, H., Szafraniec, M., Khalidov, V., Fernandez, P., Haziza, D., Massa, F., El-Nouby, A., et al.: Dinov2: Learning robust visual features without supervision. arXiv preprint arXiv:2304.07193 (2023) [3](#)

34. Redmon, J., Divvala, S., Girshick, R., Farhadi, A.: You only look once: Unified, real-time object detection. In: Proceedings of the IEEE conference on computer vision and pattern recognition. pp. 779–788 (2016) 5
35. Redmon, J., Farhadi, A.: Yolo9000: better, faster, stronger. In: Proceedings of the IEEE conference on computer vision and pattern recognition. pp. 7263–7271 (2017) 5
36. Ren, S., Luzzi, F., Lahrichi, S., Kassaw, K., Collins, L.M., Bradbury, K., Malof, J.M.: Segment anything, from space? In: Proceedings of the IEEE/CVF Winter Conference on Applications of Computer Vision. pp. 8355–8365 (2024) 3
37. Ronneberger, O., Fischer, P., Brox, T.: U-net: Convolutional networks for biomedical image segmentation. In: Medical Image Computing and Computer-Assisted Intervention–MICCAI 2015: 18th International Conference, Munich, Germany, October 5–9, 2015, Proceedings, Part III 18. pp. 234–241. Springer (2015) 11
38. Sara, R., Cvrcek, V.: Faint streak detection with certificate by adaptive multi-level bayesian inference. In: European Conference on Space Debris (2017) 4, 11
39. Su, S., Niu, W., Li, Y., Ren, C., Peng, X., Zheng, W., Yang, Z.: Dim and small space-target detection and centroid positioning based on motion feature learning. *Remote Sensing* **15**(9), 2455 (2023) 2
40. Sun, H., Bai, J., Yang, F., Bai, X.: Receptive-field and direction induced attention network for infrared dim small target detection with a large-scale dataset irdst. *IEEE Transactions on Geoscience and Remote Sensing* **61**, 1–13 (2023) 5, 11
41. Tao, J., Cao, Y., Ding, M.: Sdebrisnet: A spatial–temporal saliency network for space debris detection. *Applied Sciences* **13**(8), 4955 (2023) 5
42. Virtanen, J., Poikonen, J., Säntti, T., Komulainen, T., Torppa, J., Granvik, M., Muinonen, K., Pentikäinen, H., Martikainen, J., Näränen, J., et al.: Streak detection and analysis pipeline for space-debris optical images. *Advances in Space Research* **57**(8), 1607–1623 (2016) 2, 4
43. Wang, H., Cao, P., Wang, J., Zaiane, O.R.: Uctransnet: rethinking the skip connections in u-net from a channel-wise perspective with transformer. In: Proceedings of the AAAI conference on artificial intelligence. vol. 36, pp. 2441–2449 (2022) 11
44. Xi, J., Wen, D., Ersoy, O.K., Yi, H., Yao, D., Song, Z., Xi, S.: Space debris detection in optical image sequences. *Applied optics* **55**(28), 7929–7940 (2016) 4
45. Xue, D., Sun, J., Hu, Y., Zheng, Y., Zhu, Y., Zhang, Y.: Dim small target detection based on convolutional neural network in star image. *Multimedia Tools and Applications* **79**, 4681–4698 (2020) 2
46. Yang, X., Wu, T., Wang, N., Huang, Y., Song, B., Gao, X.: Hcnn-psi: A hybrid cnn with partial semantic information for space target recognition. *Pattern Recognition* **108**, 107531 (2020) 2
47. Yao, L., Zuo, H., Zheng, G., Fu, C., Pan, J.: Sam-da: Uav tracks anything at night with sam-powered domain adaptation. *arXiv preprint arXiv:2307.01024* (2023) 3
48. Yao, Y., Zhu, J., Liu, Q., Lu, Y., Xu, X.: An adaptive space target detection algorithm. *IEEE Geoscience and Remote Sensing Letters* **19**, 1–5 (2022) 6
49. Ying, X., Liu, L., Wang, Y., Li, R., Chen, N., Lin, Z., Sheng, W., Zhou, S.: Mapping degeneration meets label evolution: Learning infrared small target detection with single point supervision. In: Proceedings of the IEEE/CVF Conference on Computer Vision and Pattern Recognition. pp. 15528–15538 (2023) 3
50. Zhan, M., Huang, P., Zhu, S., Liu, X., Liao, G., Sheng, J., Li, S.: A modified keystone transform matched filtering method for space-moving target detection. *IEEE Transactions on Geoscience and Remote Sensing* **60**, 1–16 (2021) 2
51. Zhang, D., Yang, Q.Y., Chen, T.: Vignetting correction for a single star-sky observation image. *Applied Optics* **58**(16), 4337–4344 (2019) 2

52. Zhang, L., Rao, P., Hong, Y., Chen, X., Jia, L.: Infrared dim star background suppression method based on recursive moving target indication. *Remote Sensing* **15**(17), 4152 (2023) [2](#)
53. Zhang, M., Zhang, R., Yang, Y., Bai, H., Zhang, J., Guo, J.: Isnet: Shape matters for infrared small target detection. In: Proceedings of the IEEE/CVF Conference on Computer Vision and Pattern Recognition. pp. 877–886 (2022) [5](#)
54. Zhang, T., Cao, S., Pu, T., Peng, Z.: Agpcnet: Attention-guided pyramid context networks for infrared small target detection. arXiv preprint arXiv:2111.03580 (2021) [5, 11](#)
55. Zhang, Y., Chen, X., Rao, P., Jia, L.: Dim moving multi-target enhancement with strong robustness for false enhancement. *Remote Sensing* **15**(19), 4892 (2023) [2](#)
56. Zhu, R., Fu, Q., Liu, N., Zhao, F., Wen, G., Li, Y., Jiang, H.: Improved target detection method for space-based optoelectronic systems. *Scientific Reports* **14**(1), 1832 (2024) [2](#)